Application of ^{31}P-NMR spectroscopy to the study of striated muscle metabolism

MEYER, RONALD A., MARTIN J. KUSHMERICK, AND TRUMAN R. BROWN. *Application of ^{31}P-NMR spectroscopy to the study of striated muscle metabolism.* Am. J. Physiol. 242 (Cell Physiol. 11): C1–C11, 1982.—This review presents the principles and limitations of phosphorus nuclear magnetic resonance (^{31}P-NMR) spectroscopy as applied to the study of striated muscle metabolism. Application of the techniques discussed include noninvasive measurement of high-energy phosphate, intracellular pH, intracellular free Mg^{2+}, and metabolite compartmentation. In perfused cat biceps (fast-twitch) muscle, but not in soleus (slow-twitch), NMR spectra indicate a substantially lower (1 mM) free inorganic phosphate level than when measured chemically (6 mM). In addition, saturation and inversion spin-transfer methods that enable direct measurement of the unidirectional fluxes through creatine kinase are described. In perfused cat biceps muscle, results suggest that this enzyme and its substrates are in simple chemical equilibrium.

metabolite compartmentation; spin-transfer method; saturation-transfer method

SINCE HOULT ET AL. (29) reported the first phosphorus nuclear magnetic resonance (^{31}P-NMR) spectra of frog muscle less than a decade ago, NMR techniques have been applied to the study of systems ranging in complexity from bacterial (47) and organelle (37) suspensions to intact animals (1) and even humans (13, 41). Indeed, the clinical use of NMR, both as a probe of in situ organ metabolism and as an imaging device (27), is not far off. Yet throughout this period of phenomenal growth, striated muscle has remained the subject of the most intense interest. This focus derives in part from the fact that the phosphorylated metabolites directly measured by NMR (e.g., ATP, phosphocreatine, and inorganic phosphate) are intimately related to the function of muscle as a chemomechanical energy converter. Several reviews (5, 9, 20, 28, 39, 45) of tissue NMR have appeared recently; it is not our intention to reproduce them here. Instead, we hope to illustrate for the nonspecialist some valuable and even unique capabilities of ^{31}P-NMR spectroscopy with examples drawn from selected literature and from our own studies of arterially perfused cat skeletal muscles. Our goal is to stimulate the reader's curiosity and enthusiasm for this technique.

Pulse NMR

Biological applications of ^{31}P-NMR spectroscopy depend heavily on "pulse" techniques. Therefore, to appreciate both the uses and limitations of NMR, some familiarity with the theory and jargon of pulse techniques is required. Readable introductions to NMR theory are presented by Cantor and Schimmel (12), Farrar and Becker (17), and Gunther (25).

We begin with the fact that phosphorus nuclei are magnetic dipoles and that, when placed in a magnetic field, H, they are constrained by the laws of quantum mechanics to one of two energy levels. If we define the direction of H as the positive Z-axis (in three-dimensional coordinates), then the two energy levels correspond to two allowed orientations of the nuclear dipoles with respect to the Z-axis (Fig. 1*A*). The energy difference between the two levels is

$$\Delta E = \frac{h\gamma}{2\pi} H \qquad (1)$$

where h is Planck's constant, H is the magnetic field strength, and γ is a constant characteristic of the nucleus known as the gyromagnetic ratio. As in any other type of spectroscopy, transitions of nuclei between the two states may be induced by applying radiant energy at the appropriate resonant frequency (ν)

$$\nu = \frac{\Delta E}{h} = \frac{\gamma H}{2\pi} \qquad (2)$$

The gyromagnetic ratio is the same for all ^{31}P nuclei. The reason for the great utility of NMR is that the field, H, at a particular nucleus differs from the applied field, $H°$, by an amount that depends on the electronic structure of

0363-6143/82/0000-0000$01.25

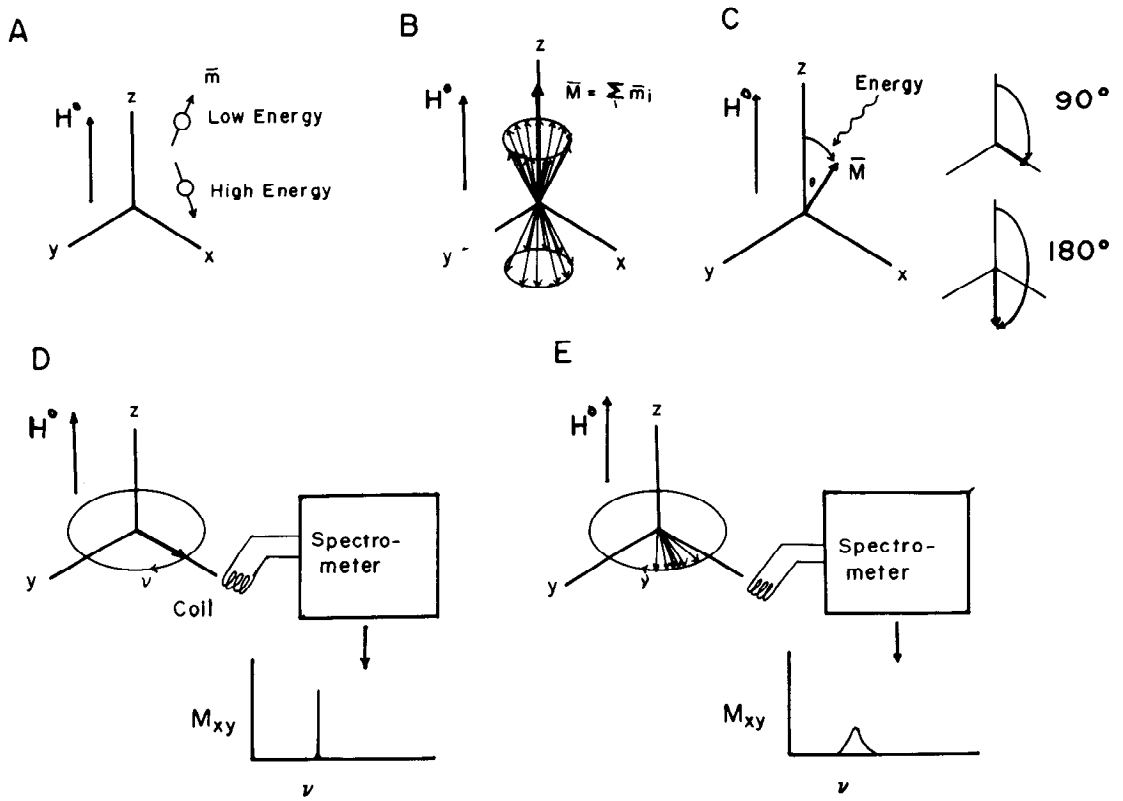

FIG. 1. Physical basis of NMR (see text).

the molecule in which the nucleus is located. Thus we can write

$$\nu = \frac{\gamma H^\circ}{2\pi}(1 - \sigma) \qquad (3)$$

where σ is the chemical shift due to the shielding of the nuclei by their molecular environment. For the compounds we will be discussing, values for σ are in the range of 10^{-5}. As σ is independent of H°, resonant frequencies are usually reported as part per million (ppm) shift relative to some convenient reference frequency.

For ^{31}P nuclei in the highest field strengths presently available (6–8 T), ν is in the 100- to 150-MHz (or radio-frequency) range, and so, compared with electronic transitions, for example, NMR transitions are induced by radiation of relatively low energy. It follows from the Boltzmann distribution that at equilibrium at biological temperatures there is only a slight excess of nuclei in the lower energy level, and therefore the capacity of a system to absorb energy by NMR is very small. This low energy absorption has two consequences. First, NMR is not a sensitive technique. Because concentrations in biological samples cannot be increased at will, it is desirable to use large tissue samples, and even then it is usually necessary to average several or even hundreds of single observations to obtain spectra with useful signal-to-noise ratios. The maximum sensitivity for ^{31}P in living tissue is about 0.2 mM using state-of-the-art technology and long times (30 min or more) for signal averaging. The second important consequence is that NMR measurements do not chemically perturb the system under study. Therefore the number of spectra that can be acquired from a single tissue is limited only by the stability of the preparation. Spectra of Langendorff-perfused hearts have been recorded for up to 7 h (23). We have developed the use of arterially perfused cat biceps and soleus muscles that are stable with respect to phosphocreatine (PCr) and ATP levels, resting oxygen consumption, and tension development for at least 12 h (30, 34).

The pulse NMR experiment is best understood in terms of the classical analysis developed by Block and embodied in a set of equations bearing his name. Consider a collection of identical nuclei in a magnetic field, H°, parallel to the positive Z axis (Fig. 1*B*). Although the nuclei can assume only two orientations with respect to H°, they are free to rotate around H°, and thus their projections may occupy any position in a circle on the X-Y plane. Therefore, in the presence of H°, the slight excess of nuclei in the lower energy level but random in the X-Y plane results in a net magnetization vector, $\boldsymbol{M}$, parallel to H°. Bloch's analysis deals with the behavior of $\boldsymbol{M}$. Without going into mathematical detail, the analysis shows that $\boldsymbol{M}$ behaves much as a gyroscope, i.e., if $\boldsymbol{M}$ is tipped relative to H°, it will rotate around H°. Its frequency of rotation is given by ν, the resonant frequency defined above (*Eq. 3*).

With this background, we present the following gross simplification of the pulse NMR experiment with apologies to our physicist friends. At equilibrium in the absence of applied radio-frequency energy, $\boldsymbol{M}$ is parallel to H° and its magnitude is proportional to the number of ^{31}P nuclei in the sample. Application of a short, broad bandwidth pulse of radio-frequency energy results in rotation of $\boldsymbol{M}$ away from the Z-axis toward the X-Y plane (Fig. 1*C*). This rotation of $\boldsymbol{M}$ away from the Z axis

corresponds to the absorption of energy by the nuclei. Therefore the extent of rotation depends on the power and duration of the pulse. By appropriate timing of a constant power pulse one can rotate $\boldsymbol{M}$ exactly into the X-Y plane, a 90° pulse. A pulse with the same radio-frequency power but twice the duration rotates $\boldsymbol{M}$ all the way to the negative Z axis, a 180° pulse. After the application of the radio-frequency pulse if there is a component of $\boldsymbol{M}$ in the X-Y plane ($\boldsymbol{M}_{xy}$), $\boldsymbol{M}$ will spin around the Z-axis at the resonant frequency defined previously (Fig. 1*D*). This motion of $\boldsymbol{M}$ in the X-Y plane induces an AC voltage in the spectrometer's detector coil with amplitude proportional to the magnitude of $\boldsymbol{M}_{xy}$ and frequency ν. The rest of the spectrometer is simply a device for generating from the coil voltage a plot of the magnitude of $\boldsymbol{M}_{xy}$ as a function of frequency—the spectrum! Specifically, the spectrum is obtained by taking the Fourier transform of the free induction decay (FID), which is a signal produced by beating the induced coil voltage against a constant reference frequency. The largest signals are obtained after a 90° pulse, because in that case $\boldsymbol{M}_{xy}$ is a maximum. A 180° pulse leaves no component of $\boldsymbol{M}$ in the X-Y plane and therefore generates no signal. If the sample contains nuclei with different chemical shifts, $\boldsymbol{M}_{xy}$ will be composed of several vectors spinning in the X-Y plane at different frequencies, and several signals will result, each with amplitude proportional to the number of nuclei with that chemical shift. Thus the small difference in chemical shift between ^{31}P nuclei in PCr and inorganic phosphate (P_i) results in separate signals. A representative FID and spectrum from a perfused cat muscle appear in Fig. 2.

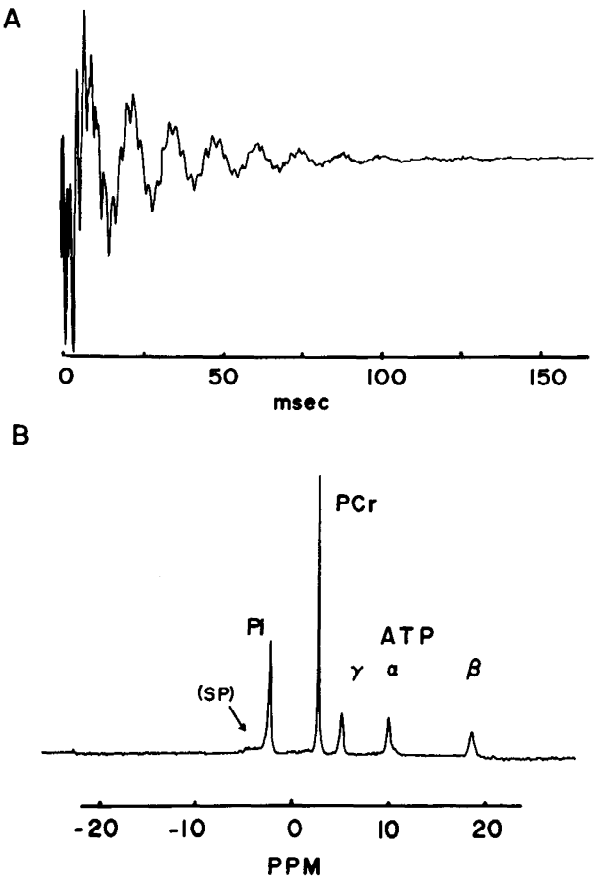

FIG. 2. *A*: Average of 400 ^{31}P-NMR free-induction decays (FID) recorded from resting, arterially perfused cat soleus muscle. Exciting pulses were 90° at 15-s intervals, sweep width ± 3,000 Hz, spectrometer frequency 109.3 MHz. Line broadening of 2 Hz was used to filter FID. Largest amplitude frequency component is due to phosphocreatine. *B*: Fourier transform of FID in *A*. Scale in ppm shift relative to frequency of 85% phosphoric acid. When present, sugar phosphate (SP) peaks would appear in region indicated. If ADP were detected in significant amounts, its α- and β-phosphate signals would overlap those from α and γ signals of ATP. Thus ATP γ signal would be greater than β. In fact, these peak areas are not significantly different. ATP α-phosphate peak also overlaps that of NAD.

Relaxation and Line Broadening

After a 90° pulse, the net magnetization, $\boldsymbol{M}$, of the sample has been disturbed from its equilibrium position along the Z axis so that it now lies in the X-Y plane. If one reconsiders the state of the individual nuclear magnetic dipoles of which $\boldsymbol{M}$ is composed, this disturbance may be separated into two components. First, there is now a component of $\boldsymbol{M}$ in the X-Y plane; hence the individual dipoles are no longer randomly distributed in the X-Y plane. Second, there is now no component of $\boldsymbol{M}$ in the Z axis; hence the distribution of nuclei between the two energy levels no longer corresponds to the equilibrium energy distribution predicted by Boltzmann's relation. The reversal of these disturbances so that $\boldsymbol{M}$ returns to its equilibrium position along the Z axis is called relaxation.

Transverse relaxation refers to the rerandomization of nuclear dipoles in the X-Y plane and determines the line width of the signal. The process may be conceived as a fanning out of the individual dipoles of $\boldsymbol{M}_{xy}$ as they spin around the Z axis (Fig. 1*E*). During this process, $\boldsymbol{M}_{xy}$ appears to the detector coil as many vectors with slightly different spinning frequencies. Therefore the spectral signal is an envelope of frequencies instead of a sharp line. The area under the envelope is the amplitude that is proportional to the number of nuclei with that particular chemical shift. Faster relaxation results in broader lines, and ideally line width = $1/\pi T_2$ where T_2 is the transverse relaxation time. As randomization proceeds, $\boldsymbol{M}_{xy}$ exponentially decays to zero with the rate constant $1/T_2$, and the induced coil voltage disappears. As the narrowest phosphorus line widths observed in living tissues are about 10 Hz, the useful data from a single scan (the FID) is generally collected within about 50–100 ms.

The mechanisms by which transverse relaxation occur (e.g., spin-spin exchange) are profoundly affected by molecular mobility, among other factors. As a general rule, decreased mobility results in faster relaxation and broader lines. Therefore signals from ^{31}P nuclei in large molecules such as DNA and phosphoproteins are so broad that they cannot be observed in living tissues by standard high-resolution NMR techniques. Similarly, the ADP bound to actin is not apparent in skeletal muscle spectra (3) (Fig. 2). The practical result of this, together with the low sensitivity of NMR, is that the only signals resolved in ^{31}P-NMR spectra of striated muscles are from relatively low-molecular-weight compounds present at millimolar levels in free solution, e.g. ATP, PCr, P_i, sugar phosphates, and occasionally phosphodiesters (5, 29).

We should mention that the observed line widths of signals from living tissues are always much broader than predicted on the basis of T_2 measurements. For example, in perfused soleus muscle, the PCr line width is about 10 Hz (corresponding to an effective T_2, i.e., T_2^*, of 30 ms), but the true T_2 [measured by the Carr-Purcell-Gill-Meiboom technique (17)] is 0.25 s. This additional line broadening results from randomization of $\boldsymbol{M}_{xy}$ due to inhomogeneity of the main field. The effect can be reduced by physically spinning the sample; unfortunately, this is impractical for perfused tissues. We have also ignored the phenomena of homo- and heteronuclear spin-spin coupling, which leads to signal splitting. For example, the signal from the β-phosphate of ATP is actually a triplet because of spin coupling with the phosphorus nuclei in the adjacent phosphate groups. Because the line widths of signals achievable with intact organs are so broad, this fine structure is not generally resolved. The interested reader is referred to the texts cited above.

Longitudinal relaxation refers to recovery of the equilibrium Boltzmann distribution of nuclei between the two energy levels and corresponds to the recovery of net magnetization along the Z axis. This requires transfer of the absorbed energy from the excited nuclei to their surroundings and is typically much slower than transverse relaxation. In fact, when T_2 is very short, $\boldsymbol{M}_{xy}$ may decay to zero before any appreciable magnetization reappears along the Z axis. At this point, when there is no net magnetization, the two energy levels are equally populated and the system is said to be saturated. It should be clear that application of another 90° pulse at this point would result in no signal. The recovery of magnetization along the Z axis (M_z) is a first-order process described by

$$\frac{dM_z}{dt} = \frac{M_z^\circ - M_z}{T_1} \qquad (4)$$

where M_z° is the magnitude of $\boldsymbol{M}$ at equilibrium and T_1 is the longitudinal relaxation time. T_1 values are typically around 0.5–3 s for the ^{31}P nuclei observed in living tissue.

The above discussion reveals that the spectral signals obtained after a 90° pulse will not necessarily be proportional to the number of nuclei in the sample unless the nuclear system is initially at equilibrium, so that $M_z = M_z^\circ$. However, the signals after a 90° pulse are always a measure of M_z immediately before the pulse. For example, consider a 180° pulse, which rotates $\boldsymbol{M}$ from the positive to the negative Z axis. This corresponds to inversion of the nuclear energy distribution so that there are more nuclei in the higher than the lower energy state. After such a pulse, $\boldsymbol{M}$ will relax to its equilibrium position along a time course described by *Eq. 4*. However, if a 90° pulse is applied soon after the 180° pulse, the inverted magnetization will be further rotated into the X-Y plane. (Based on quantum mechanics, this corresponds to the stimulated emission of energy from the nuclei, analogous to the principle of lasers.) The component $\boldsymbol{M}_{xy}$ then rotates in the X-Y plane at its characteristic resonant frequency and induces a coil voltage as before. However, this voltage is 180° out of phase from that induced by the magnetization that follows a single 90° pulse. Therefore the Fourier-transformed FID gives an inverted spectral signal. If one repeats this experiment with different delay times between the 180° and 90° pulse, one can follow the exponential recovery of M_z toward equilibrium. This "180°-delay-90°" sequence is a standard technique for determining T_1, the inversion-recovery experiment.

As mentioned above, useful spectra are usually obtained by averaging together several or even hundreds of FID's or scans. Unfortunately, longitudinal relaxation limits the rate at which successive scans can be accumulated, because M_z does not completely recover if pulses are applied too closely together, i.e., the signals become partially saturated. Because the T_1 of nuclei in different molecules may be different, the relative degree of saturation for each signal may differ, and therefore signal amplitudes measured under partial saturation conditions will not be proportional to the number of nuclei in each species. The safest procedure is to assure that equilibrium is reestablished by collecting scans at intervals no less than five times the longest T_1, or every 15 s in muscle. If this is not practical, for example due to instability of the preparation, one can use shorter pulse widths so that $\boldsymbol{M}$ returns to equilibrium sooner than after a 90° pulse. Furthermore, if the T_1 are thought to be constants, one can correct for differing partial saturation of the signals. However, this procedure ignores the possibility that the T_1 of some species may change during an experiment due, for example, to binding or exchange of phosphate groups during contraction. Fortunately the time resolution of an NMR experiment is not necessarily limited by the rate of spectrum accumulation. If the physiological events of interest are repeatable, as are heart and muscle contraction, one can time the pulses to the particular point of interest, the gated NMR experiment (19, 21). In that case, the time resolution of NMR experiments is limited only by the time required to record a single FID, about 50 ms.

Applications to Muscle Physiology

As one might guess by examination of the spectrum in Fig. 2, the most immediate application of ^{31}P-NMR is determination of the relative levels of PCr, ATP, and P_i in intact muscles. In practice it is difficult to calibrate signal areas in terms of absolute tissue concentrations. Instead relative areas are usually measured and scaled by reference to chemical analysis of the same tissue (see below). The various peaks have been identified by comparison with model solutions. In stimulated or ischemic muscles sugar phosphate peaks also appear (11, 15), and some muscles have exhibited peaks due to previously ignored phosphodiesters, which appear to be species specific and may have some relation to muscle pathology (4, 5, 10).

If measurements of these few metabolites were the only use of ^{31}P-NMR it would still be a valuable new technique because the measurements can be made repeatedly on the same muscle. Thus it is now fairly routine to observe the changes in PCr, ATP, and P_i during a sequence of contractions (Figs. 3 and 4) or during an ischemic period by NMR (22, 24, 38). However, the unique power of NMR lies in its use as a probe of the intracellular environment. As an illustration of this

power, consider a calculation of the so-called phosphorylation potential

$$\Gamma = \frac{[ATP]}{[ADP][P_i]}$$

which, together with pH, determines the free energy of hydrolysis of ATP in vivo and may be a key parameter in the control of energy metabolism, ion transport, and contractile properties (16, 48). This calculation requires accurate assessment of the cytoplasmic concentrations of ATP, ADP, and P_i. Unfortunately, the chemically measured levels of these metabolites may not accurately reflect their true cytoplasmic levels. This is certainly the case for the ADP in muscle, as the chemical measurement includes ADP tightly bound to actin and perhaps other proteins. The usual practice is to calculate the level of ADP from the assumed equilibrium of the creatine kinase reaction (32, 48)

$$PCr^{-2} + MgADP^{-1} + H^{+1} \leftrightarrow Cr + MgATP^{-2}$$

This in turn requires estimation of the apparent equilibrium constant for creatine kinase in vivo, which depends on both pH and the free Mg^{2+} concentration (31). ^{31}P-NMR offers insight into each of these questions.

Metabolite compartmentation and binding. The original observation (29) that the relative levels of PCr, ATP, and P_i in frog muscle determined by NMR agreed with chemical analysis provided the first direct evidence that these metabolites exist predominantly in free solution in vivo. On the other hand, the failure to observe ADP by NMR (free concn < 0.2 mM) confirms the expectation [based on calculations of enzymatic reaction equilibria (48)] that the free ADP level in muscle is less than that measured chemically (about 0.8 mM). This difference is commonly attributed to binding of most of the chemically measured ADP by actin in vivo (44). The fact that in liver the chemically measured ADP (0.5 mM) is resolved by NMR (33) confirms this view.

In well-oxygenated mammalian muscles, NMR data suggest that the free P_i level is also substantially less than that determined chemically (1). We find this discrepancy is particularly evident in the cat biceps, a predominantly fast-twitch muscle (Table 1). The data cannot as yet statistically exclude the possibility that this reflects, in part, the artifactual hydrolysis of PCr during freezing and extraction for chemical analysis. Another possibility is that up to 4 μmol/g of the chemically measured phosphate exists in an unidentified bound state in the muscle. In either case, the results suggest that the true free inorganic phosphate level in resting fast-twitch muscle is severalfold lower than the 6–8 mM commonly assumed on the basis of chemical assays. As a number of enzymes [e.g., phosphofructokinase (46) and AMP deaminase (49)] are allosterically sensitive to P_i in the 1-mM range, the potential role of P_i in the regulation of metabolism ought to be reinvestigated.

TABLE 1. *Metabolite contents in cat skeletal muscles measured chemically and by ^{31}P-NMR*

	Chemical Assay	NMR Assay
	Biceps (fast twitch)	
ATP	7.0 ± 0.3	7.0
PCr	20.8 ± 0.9	22.0 ± 2.0
Cr	6.9 ± 0.6	
P_i	5.6 ± 0.9	0.9 ± 0.3
	Soleus (slow twitch)	
ATP	3.7 ± 0.3	3.7
PCr	11.7 ± 0.3	13.2 ± 1.4
Cr	6.1 ± 0.8	
P_i	9.2 ± 0.8	6.1 ± 0.3

Values are mean ± SE (n = 4) given in μmol/g wet wt. P_i, inorganic phosphate. Chemical assays were of perchloric acid extracts by standard enzymatic techniques. NMR peak areas were normalized to mean ATP level measured by chemical analysis.

Intracellular pH

Moon and Richards (35) pioneered the use of ^{31}P-NMR for determination of intracellular pH using red blood cells. The method relies on the fact that the chemical shifts of phosphate signals are exquisitely sensitive to pH in the regions around their pK_a. In the biological range of pH 6.2–7.4, the inorganic phosphate signal (pK_a 6.8) proves most valuable for this purpose. Measured relative to the PCr signal, which is insensitive to pH in this range (pK_a 4.5), the chemical shift of P_i ranges from 5.3 ppm (at pH 7.4) to 3.9 (pH 6.2). The accuracy of the method depends on the construction of titration curves of the phosphate chemical shift in solutions designed to mimic the intracellular environment with respect to ionic strength, temperature, and so on (10). However, because the relative position of signals can be measured to better than 0.02 ppm, relative shifts in intracellular pH can be measured with extraordinary precision in intact tissue, and, in this respect, NMR must be considered superior to microelectrode or weak base distribution methods (40). The pH measured by NMR will naturally reflect the pH in whatever intracellular compartments contain the phosphate observed. Recent work by Bailey et al. (2), who calculated the same pH from chemical shifts of inorganic phosphate and phosphorylated 2-deoxyglucose, strongly argues that this is the cytoplasmic compartment in striated muscle cells.

Despite some earlier confusion about the pH in perfused hearts (43), most NMR data available indicate that the cytoplasmic pH in well-oxygenated heart and skeletal muscle is 7.0–7.2. The expected decreases in pH associated with lactate accumulation during contraction or ischemia have been observed in both heart and skeletal muscle (15, 22, 24, 38, 51). Conversely, we have observed alkalinization (from pH 7.1 to 7.3) associated with PCr hydrolysis during mild contraction of the cat soleus, a muscle with low glycolytic capacity (30). Alkalinization was also reported during forearm exercise in a patient with McArdle's disease (41).

Unlike weak acid or base distribution methods, NMR can also provide information about the pH distribution in cells and tissues. For example, line broadening or actual splitting of the inorganic phosphate peak has been observed in some muscles during anoxia or ischemia (11, 51). This may indicate the existence of microcompartments with differing pH within the cytoplasm. However, it is difficult to sort out the contribution of cell to cell

heterogeneity to peak broadening. We have not observed significant peak broadening during contraction (Fig. 3) or ischemia in the cat soleus, which consists almost entirely of slow-twitch oxidative fibers. In contrast, P_i peak broadening is readily apparent in the cat biceps (Fig. 4), which contains a more heterogenous fiber population (70% fast-twitch glycolytic, 24% fast-twitch oxidative-glycolytic, 6% slow-twitch oxidative).

Intracellular Free Mg^{2+}

Among the earliest results of the application of ^{31}P-NMR to biochemistry was the observation that the chemical shifts of the ATP phosphate signals depend on the fraction of ATP complexed with Mg^{2+} (14). Thus Hoult et al. (29) concluded in their original report that over 90% of the ATP in frog muscle exists as the Mg^{2+} complex. One can calculate the free intracellular Mg^{2+} level from these data if the Mg ATP dissociation constant is accurately known under intracellular conditions. By this method, Gupta and Moore (26) estimated that the free Mg^{2+} level in frog skeletal muscle is 0.6 mM. Using a different effective dissociation constant, Wu et al. (50) estimated a free Mg^{2+} level of 2.5 mM in frog muscle and guinea pig hearts. Unfortunately, the binding constant of ADP for Mg^{2+} (0.7 mM) lies in the disputed range, and therefore this difference has a significant effect, for example, on the apparent equilibrium constant of creatine kinase (31). Both groups found that the calculated free Mg^{2+} level was unchanged by physiological interventions such as ischemia or insulin treatment, suggesting that Mg^{2+} levels are well buffered in vivo.

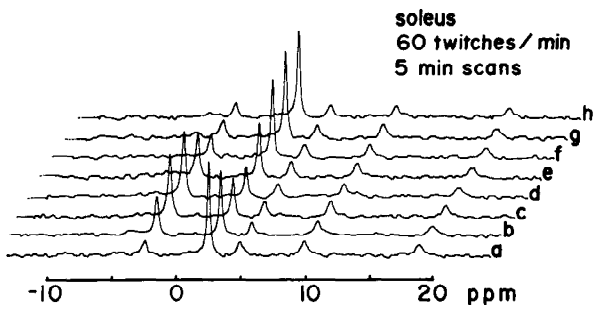

FIG. 3. Stimulation-recovery cycle showing ^{31}P-NMR spectra of cat soleus muscle before (*a*) during (*b–d*), and after (*e–h*) 15 min of isometric stimulation at 60 twitches/min. Each spectrum is average of 20 scans accumulated after 90° pulses at 15-s intervals (10-Hz line broadening). Thus each spectrum represents average over 5-min period. Successive spectra are shifted about 1 ppm to right to aid viewing.

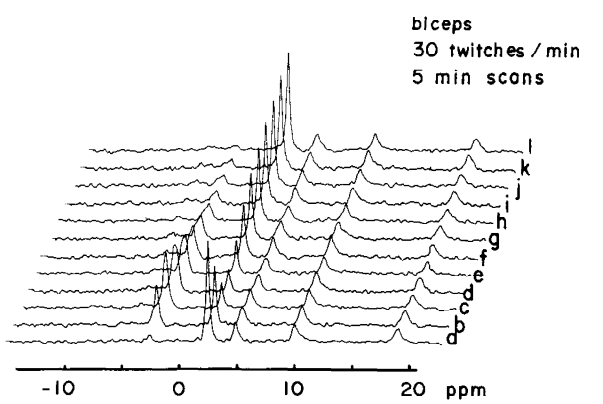

FIG. 4. Stimulation-recovery cycle showing ^{31}P-NMR spectra of cat biceps muscle before (*a*), during (*b–d*), and after (*e–l*) 15 min of isometric stimulation at 30 twitches/min. Collection parameters as in Fig. 3.

If we accept 2 mM as the free Mg^{2+} level in resting muscle, then the apparent equilibrium constant of creatine kinase at pH 7.1 is (31)

$$K' = \frac{[ATP]\,[Cr]}{[ADP]\,[PCr]} = 140$$

where the bracketed terms are the total free reactant concentrations, assuming 70% of the muscle weight is intracellular fluid. Applying the NMR data of Table 1, one calculates a free ADP level of 22 μM in resting cat biceps. Thus the calculated phosphorylation potential is $3.5 \times 10^5\ M^{-1}$, which is over 10-fold higher than previously calculated for mammalian fast-twitch muscle based on chemical measurements alone (48).

Direct Measurement of in vivo Reaction Rates by NMR

Calculation of the free ADP in the above example relied on the assumption that the creatine kinase reaction is at or near equilibrium and that the cytosol may be considered a well-mixed solution as far as this reaction is concerned. The assumption that this or any reaction is actually at a simple chemical equilibrium has depended on two experimental approaches. In the first, one measures the total contents of the reactants in tissue samples frozen under various conditions and calculates a mass action ratio. If the calculated ratio is always nearly equal to the equilibrium constant determined in solutions mimicking intracellular conditions, then equilibrium is assumed. This approach is not directly applicable to creatine kinase, because one cannot directly measure the free ADP. In the second approach, one measures the total activity of the enzyme in extracts of tissue incubated with physiological levels of modulators. If the measured activity substantially exceeds the maximum flux thought to occur in vivo, then equilibrium is assumed. Unfortunately this approach neglects the possibility that the intracellular localization of the enzyme or substrates might severely modify the reaction in vivo. Creatine kinase is known to bind to mitochondria, membranes, and myofibrils, and it has been proposed that this localization is crucial to the enzyme's function in an energy shuttle (6, 42).

It is possible to measure directly the unidirectional rates of certain reactions in vivo using NMR spin-transfer techniques. By comparing the rates in vivo with those measured in vitro in equilibrium solutions containing the same enzyme and substrate concentrations, one could in principle directly determine the intracellular status of the reaction. The remaining discussion will introduce the theory of these spin-transfer methods and summarize recent results of their application to the creatine kinase reaction in striated muscle.

Two methods, saturation and inversion transfer, have been developed. Each depends on the selective perturbation of the nuclei in one molecular species from their

equilibrium energy distribution. If there is chemical exchange of nuclei to a second molecular species before longitudinal relaxation is complete, then the perturbation will also appear in the second species. In saturation transfer, originally developed by Forsen and Hoffmann (18) in 1963, the perturbation is selective saturation of one species signal by continuous irradiation at its precise resonant frequency. As a result, there is no net magnetization due to this species, and no signal appears from it in a spectrum obtained after the usual broad bandwidth 90° pulse (Fig. 5). Inversion transfer, first applied to enzyme kinetics by Brown and Ogawa (8), is a modification of the standard T_1 inversion-recovery experiment. In this case the perturbation is selective inversion of one species' signal by application of a narrow bandwidth 180° pulse before the usual 90° pulse (Fig. 6). In both cases chemical exchange results in a decrease in the signal of the second molecular species.

Quantitative estimation of reaction rates from spin-transfer experiments like those shown in Figs. 5 and 6 is facilitated by several simplifying assumptions. Let us consider the creatine kinase (CK) reaction as a psuedo-first-order exchange of phosphate between PCr and the γ-phosphate of ATP

$$\mathrm{PCr} \underset{K_2}{\overset{K_1}{\rightleftarrows}} \mathrm{ATP}$$

We will assume that this reaction is at chemical equilibrium and that neither species exchanges phosphate with any other species to a significant extent. Further, we will assume that there is no compartmentation of reactants, so that the levels of PCr and ATP determined by ^{31}P-NMR are indeed proportional to the concentrations involved in the reaction. These last three assumptions seem likely to be correct for equilibrium solutions of CK and its reactants in vitro but remain to be confirmed in vivo. Accepting them for the moment, we may write:

$$M^{\circ}_{\mathrm{PCr}} K_1 = M^{\circ}_{\mathrm{ATP}} K_2 \qquad (5)$$

where M°_{PCr} and M°_{ATP} are the net magnetizations due to each species when they have obtained their Boltzmann equilibrium energy distributions. Finally, we modify *Eq. 4* describing the longitudinal relaxation of the net magnetization of each species to account for chemical exchange between the species

$$\frac{dM_{\mathrm{PCr}}}{dt} = \frac{M^{\circ}_{\mathrm{PCr}} - M_{\mathrm{PCr}}}{T_{1\,\mathrm{PCr}}} - K_1 M_{\mathrm{PCr}} + K_2 M_{\mathrm{ATP}} \qquad (6)$$

$$\frac{dM_{\mathrm{ATP}}}{dt} = \frac{M^{\circ}_{\mathrm{ATP}} - M_{\mathrm{ATP}}}{T_{1\,\mathrm{ATP}}} - K_2 M_{\mathrm{ATP}} + K_1 M_{\mathrm{PCr}} \qquad (7)$$

where the T_1's are those that would be measured in the absence of exchange. The reader should note that *Eq. 4* is not valid for this exchanging system.

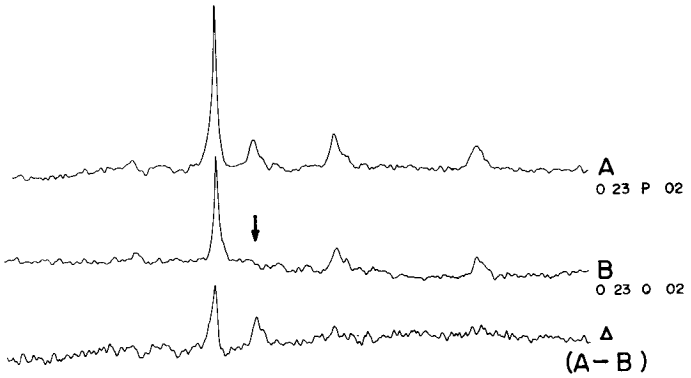

FIG. 5. ^{31}P-NMR spectra of perfused cat biceps muscle before (*A*) and after (*B*) selective saturation of γ-ATP phosphate signal by continuous low power irradiation. *Arrow* indicates frequency of the selective irradiation. *Bottom spectrum* is difference (A − B) and shows complete saturation of γ-ATP and transfer to PCr. Other collection parameters as in Fig. 3.

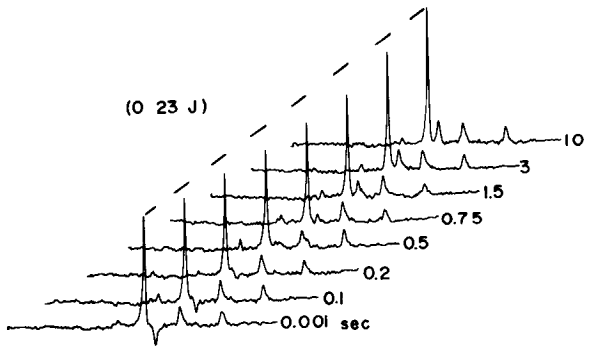

FIG. 6. Example of ATP γ-phosphate inversion transfer experiment in cat biceps. Spectra were accumulated as follows. First low-power 180° selective inverting pulse was applied at frequency of ATP-γ. Nuclei were then unperturbed for delay time (given at right of each spectrum) to allow inverted nuclei to mix. After this delay, usual high-power, broad bandwidth 90°-pulse was applied. Nuclear system was then given 15 s to recover and process repeated until 20 scans were accumulated for each delay time. *Dashed line* connects PCr peaks to emphasize decrease in magnetization due to transfer of inverted nuclei from ATP. As described in text, time course of this decrease is measure of unidirectional flux through creatine kinase.

Saturation Transfer

Consider the selective saturation of the signal of γ-phosphate from ATP.
Then $M_{\mathrm{ATP}} = 0$, and *Eq. 6* becomes

$$\frac{dM_{\mathrm{PCr}}}{dt} = \frac{M^{\circ}_{\mathrm{PCr}} - M_{\mathrm{PCr}}}{T_{1\,\mathrm{PCr}}} - K_1 M_{\mathrm{PCr}} \qquad (8)$$

This has the solution

$$M_{\mathrm{PCr}} = M^{\circ}_{\mathrm{PCr}}/(1 + K_1 T_{1\,\mathrm{PCr}}) + C \exp[-(1/T_{1\,\mathrm{PCr}} + K_1)t] \qquad (9)$$

where C is a constant. Therefore, after saturation of ATP, the PCr signal decreases exponentially with rate constant

$$\frac{1}{\tau} = \left(\frac{1}{T_{1\,\mathrm{PCr}}} + K_1\right) \qquad (10)$$

and reaches a steady-state level at $t = \infty$ of

$$M_{\mathrm{Pcr}}\,|_{\,t=\infty} = M^{\circ}_{\mathrm{PCr}}/(1 + K_1 T_{1\,\mathrm{PCr}}) \qquad (11)$$

Therefore the decrease in the PCr signal during saturation of ATP provides a measure of K_1, the unidirectional rate constant for exchange of phosphate from PCr to ATP. If T_1 for PCr is known, then the rate constant K_1

can be directly calculated from *Eq. 11* and the flux from PCr to ATP from

$$\text{flux} = K_1 M^{\circ}_{PCr} = K_1[PCr] \quad (12)$$

If T_1 is not known, one can follow the exponential decrease in M_{PCr} after the application of saturating radiation of ATP and determine $1/\tau$. Both K_1 and the T_1 for PCr may then be calculated by simultaneous solution of *Eqs. 10* and *11*. By analogous reasoning, one can calculate K_2 and the unidirectional flux from ATP to PCr from the decrease in ATP signal after saturation of PCr.

Inversion Transfer

Now consider the selective inversion of ATP. Immediately after the inverting pulse, at $t = 0$, no relaxation or exchange of inverted nuclei has yet occurred, and therefore $M_{ATP} = -M^{\circ}_{ATP}$, and $M_{PCr} = M^{\circ}_{PCr}$ (assuming perfect inversion). Applying these boundary conditions to *Eq. 6*, one arrives at a solution of the form

$$M_{PCr} = M^{\circ}_{PCr}(1 - A \exp[-C_1 t] + A \exp[-C_2 t]) \quad (13)$$

where A, C_1, and C_2 are constants that include the terms K_1, K_2, and the T_1 for both PCr and ATP. Thus, following inversion of ATP, the PCr signal will decrease, pass through a minimum, and then return to its equilibrium value (Fig. 6). By suitable curve fitting, one could in principle evaluate the unknown terms from data like that in Fig. 6. However, by applying our simplifying assumptions, a more expedient analysis results. Directly entering the boundary conditions at $t = 0$ into *Eq. 6*, one arrives at:

$$\left.\frac{dM_{PCr}}{dt}\right|_{t=0} = -(K_1 M^{\circ}_{PCr} + K_2 M^{\circ}_{ATP}) \quad (14)$$

The terms in parentheses are just the sum of the two unidirectional fluxes through CK. If the reaction is at equilibrium, then these are equal (*Eq. 5*) and

$$K_1 M^{\circ}_{PCr} = \tfrac{1}{2}\left(\left.\frac{dM_{PCr}}{dt}\right|_{t=0}\right) \quad (15)$$

Therefore the initial rate of decrease in the PCr signal after inversion of ATP is a measure of the unidirectional flux through CK. By analogous reasoning, in this equilibrium system, one can calculate the same flux from the rate of decrease in ATP signal after selective inversion of PCr.

Now consider any steady-state system containing creatine kinase and its reactants. If all of the assumptions used in the above derivations are correct, then *1*) saturation and inversion transfer experiments should yield the same results, and *2*) the flux calculated from inversion or saturation of ATP should equal that calculated after inversion or saturation of PCr. A simple equilibrium solution of CK and its reactants in vitro appears to be such a system, inasmuch as both of these statements are correct within the experimental error at about 10% (Table 2). Our preliminary data also indicate that, within experimental error, these statements are correct for the resting cat biceps muscle (30). On this basis, we concluded that in fast-twitch muscle, the entire cellular contents of ATP and PCr may be considered to be in simple chemical equilibrium via the CK reaction. Gadian et al. (21) reached a similar conclusion from saturation transfer measurements of CK flux in resting frog muscle.

If the activity of CK is not modified by its localization in the cell, then the flux measured in vivo should also equal that measured in model solutions containing the same specific activity of enzyme. Figure 7 shows the CK flux measured by inversion transfer in a model solution designed to mimic the intracellular environment. Also plotted are data from the cat biceps (30). We feel that, given the difficulty in mimicking precisely the intracellular environment, there is good agreement in the data. Therefore we conclude that, so far as CK and its reactants are concerned, the cytosol of fast-twitch muscle cannot be distinguished from a simple, well-mixed solution.

Comparison and Limitations of Spin-transfer Methods

Despite the results shown in Table 2, saturation and inversion transfer are not equivalent methods. This is illustrated by the following example. Suppose that ATP were compartmentalized so that only some fraction, f, of

TABLE 2. *Creatine kinase unidirectional fluxes measured in vitro by saturation and inversion transfer*

	Flux PCr → ATP	Flux ATP → PCr
Saturation	9.5	7.2
Inversion	9.5	9.0

Values are in $\mu mol \cdot ml^{-1} \cdot s^{-1}$. Solution at pH 7.0 and 28°C contained (in mM) PCr 25, ATP 8, Cr 3, Na^+ pipes 50, K^+ acetate 50, Mg^{2+} acetate 10, mercaptoethanol 0.5, as well as 10 μM ethylenediaminetetraacetic acid (EDTA), 0.5 mM mercaptoethanol, 1 mg/ml bovine serum albumin, and 26.6 mg/ml crystalline rabbit creatine kinase.

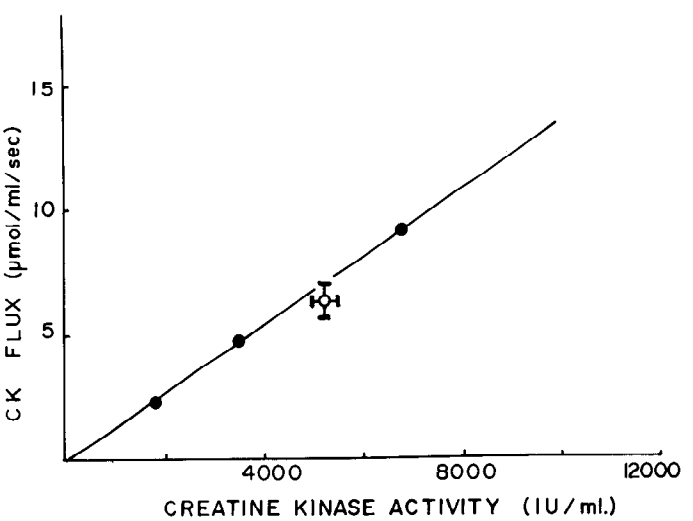

FIG. 7. Creatine kinase unidirectional flux calculated from ATP inversion transfer experiments in vitro (●) and in resting cat biceps muscle (○) (*bars* ± SE). In vitro solution contained 25 mM PCr, 8 mM ATP, 3 mM Cr, 50 mM Na^+ imidazole, 10 mM $MgSO_4$, 10 mM NaCl, 100 mM K acetate, 50 μM ethylenediaminetetraacetic acid (EDTA), 0.5 mM mercaptoethanol, and 1 mg/ml bovine serum albumin, pH 7, 28°C. Data for biceps (mean ± SE, $n = 5$) from Ref. 30 converted to mM assuming 70% of muscle mass is intracellular fluid. Creatine kinase activity was assayed in muscle homogenates by the method of S. B. Rosalki, *J. Lab. Clin. Med.* 69: 696–705, 1967.

the total ATP measured by NMR actually takes part in the CK reaction. Suppose further that this fraction is in chemical equilibrium with the entire pool of PCr

$$\mathrm{PCr} \underset{K_2}{\overset{K_1}{\rightleftarrows}} \mathrm{f\,ATP}$$

$$M^{\circ}_{\mathrm{PCr}} K_1 = \mathrm{f} M^{\circ}_{\mathrm{ATP}} K_2 \qquad (16)$$

where $0 < \mathrm{f} < 1$. The longitudinal relaxation equations modified for this exchange are

$$\frac{\mathrm{d}M_{\mathrm{PCr}}}{\mathrm{d}t} = \frac{M^{\circ}_{\mathrm{PCr}} - M_{\mathrm{PCr}}}{T_{1\,\mathrm{PCr}}} - K_1 M_{\mathrm{PCr}} + K_2 M_x \qquad (17)$$

$$\frac{\mathrm{d}M_{\mathrm{ATP}}}{\mathrm{d}t} = \frac{M^{\circ}_{\mathrm{ATP}} - M_{\mathrm{ATP}}}{T_{1\,\mathrm{ATP}}} - K_2 M_x + K_1 M_{\mathrm{PCr}} \qquad (18)$$

where M_x denotes the net magnetization due to the exchanging fraction of ATP. If the nuclei are in their Boltzmann equilibrium energy distribution, then $M_x = M^{\circ}_x = fM^{\circ}_{\mathrm{ATP}}$.

Now consider the results of saturation transfer experiments on this system. When ATP is saturated, the magnetization due to both the exchanging and nonexchanging fractions of ATP become zero. Therefore *Eqs. 8–11* are still valid, and the rate constant for exchange from PCr to ATP may still be calculated from *Eq. 11*. However, when PCr is saturated, only the exchanging fraction of ATP will receive saturated nuclei. Therefore the relative decrease in the ATP signal will be erroneously small, and the analog of *Eq. 11*

$$M_{\mathrm{ATP}}|_{t=\infty} = M^{\circ}_{\mathrm{ATP}}/(1 + K_2 T_{1\,\mathrm{ATP}}) \qquad (19)$$

will not be correct. The correct solution for this system after saturation of PCr is

$$M_{\mathrm{ATP}} = M^{\circ}_{\mathrm{ATP}} \frac{(1 + K_2 T_{1\,\mathrm{ATP}}(1 - \mathrm{f}))}{(1 + K_2 T_{1\,\mathrm{ATP}})} + C \exp\left[-\left(\frac{1}{T_{1\,\mathrm{ATP}}} + K_2\right) t\right] \qquad (20)$$

In fact, one can show that direct application of *Eq. 19* to this system using a value for the T_1 of ATP obtained by the standard inversion recovery experiment would result in underestimation of the flux from ATP to PCr. Therefore saturation transfer experiments on this system could lead to the false conclusion that the two unidirectional fluxes were not the same. (On the other hand, from *Eq. 20*, the analog of *Eq. 10* would be correct for this system. Therefore, simultaneous solution of the analogs of *Eqs. 10* and *11* would yield the correct flux, but the T_1 so calculated would be underestimated. Therefore the T_1 calculated from a selective progressive saturation experiment would be less than that calculated from a standard inversion recovery experiment.)

Now consider the results of inversion transfer experiments on the same system. Again, inversion of ATP inverts both fractions and at $t = 0$, $M_{\mathrm{PCr}} = M^{\circ}_{\mathrm{PCr}}$ and $M_x = -M^{\circ}_x = -fM^{\circ}_{\mathrm{ATP}}$. Applying these conditions to *Eq. 17* at $t = 0$ and substituting *Eq. 16*, one derives the correct expressions

$$\left.\frac{\mathrm{d}M_{\mathrm{PCr}}}{\mathrm{d}t}\right|_{t=0} = -(K_1 M^{\circ}_{\mathrm{PCr}} + K_2 \mathrm{f} M^{\circ}_{\mathrm{ATP}}) = -2(K_1 M^{\circ}_{\mathrm{PCr}}) \qquad (21)$$

On the other hand, inversion of PCr can only affect the exchanging fraction of ATP. Therefore *Eq. 18* may be modified to

$$\frac{\mathrm{d}M_{\mathrm{ATP}}}{\mathrm{d}t} = \frac{\mathrm{d}M_x}{\mathrm{d}t} = \frac{M^{\circ}_x - M_x}{T_{1\,\mathrm{ATP}}} - K_2 M_x + K_1 M_{\mathrm{PCr}} \qquad (22)$$

But immediately after the inverting pulse $M_{\mathrm{PCr}} = -M^{\circ}_{PCr}$ and $M_x = M^{\circ}_x = \mathrm{f} M^{\circ}_{\mathrm{ATP}}$, so at $t = 0$

$$\left.\frac{\mathrm{d}M_{\mathrm{ATP}}}{\mathrm{d}t}\right|_{t=0} = -(K_1 M^{\circ}_{\mathrm{PCr}} + K_2 \mathrm{f} M^{\circ}_{\mathrm{ATP}}) \qquad (23)$$

Therefore inversion of ATP or PCr in this system would result in the same (*Eq. 21*) calculated fluxes using our expedient analysis. This analysis of the inversion transfer experiment utilizes only data from the initial slope of the change in magnetization of the noninverted species. In principle, a complete analysis of data like that shown in Fig. 6 could detect that only a fraction of the total ATP was taking part in the exchange. We are now developing computer programs to perform this more sophisticated analysis to extract the maximum possible information from a set of inversion transfer measurements.

Two groups (7, 36) have applied saturation transfer methods to the CK reaction in perfused rodent hearts. Both found that the measured unidirectional flux from ATP to PCr is less than that from PCr to ATP, despite that fact that the system is in a steady state. Nunnally and Hollis (36) suggested that this paradox could be explained by intracellular compartmentation of the reactants. Gadian and co-workers (7, 20) seem inclined toward the possibility of exchange of ATP phosphate to other as yet unidentified molecules. The only firm conclusion warranted at present is that one or more of the assumptions upon which the standard, simple analysis is based are wrong. It is hoped that application of both inversion and saturation methods, under varying physiological conditions, will ultimately clarify this situation.

Finally we should point out that the low sensitivity of NMR limits the application of spin-transfer methods to relatively fast chemical exchanges. For example, suppose that the smallest decrease one can reliably detect in a signal is 5%. Then from *Eq. 11*, the slowest unidirectional rate constant one can measure by saturation transfer is

$$K = \frac{1}{T_1}(0.05) \qquad (24)$$

or about 0.05/s, assuming T_1 is 1 s. For ATP in the cat biceps muscle, this would correspond to a unidirectional flux of around 0.3 $\mathrm{mol \cdot g^{-1} \cdot s^{-1}}$. This is over 30-fold greater than the resting net ATPase rate in this muscle (0.5 $\mathrm{mol \cdot g^{-1} \cdot min^{-1}}$ based on the resting O_2 consumption at 30°C and assuming P/O_2 equals 6.2). Therefore decreases in the ATP signal during saturation of P_i have not been observed in this muscle. Conversely, decreases in P_i signal have not been reported during saturation of ATP in contracting frog muscle or perfused hearts. The inversion

method is subject to the same limitation, because if the reaction rate constants are much smaller than $1/T_1$, the inverted nuclei will return to their equilibrium energy distribution before significant exchange can occur. Despite this limitation, we feel that these methods offer unique power as direct, noninvasive probes of cellular metabolism.

In summary, ^{31}P-NMR is already an important tool for the study of metabolism. Spectra can be recorded for many hours from stable tissue preparations, allowing routine, noninvasive measurement of high energy phosphates. Transient changes in intracellular pH can be observed. Direct estimation of intracellular reaction rates is possible and thereby provides unique information in intact cells and tissues. With this range of applications, ^{31}P-NMR seems likely to become an even more important research and clinical tool in the near future.

The high field NMR experiments were performed at the NMR Facility for Biomolecular Research located at the F. Bitter National Magnet Laboratory, Massachusetts Institute of Technology. The NMR Facility is supported by Grant RR-00995 from the Division of Research Resources of the National Institutes of Health and by the National Science Foundation under Contract C-670. Portions of this research not done at Bell Laboratories were supported by Grant AM-14485 from the National Institutes of Health, by a grant from the Muscular Dystrophy Association of America, and by Research Career Development Award AM-00178 to M.J. Kushmerick. R.A. Meyer was supported by a postdoctoral fellowship from the Muscular Dystrophy Association of America.

REFERENCES

1. ACKERMAN, J. J. H., T. H. GROVE, G. G. WONG, D. G. GADIAN, AND G. K. RADDA. Mapping of metabolites in whole animals by ^{31}P-NMR using surface coils. *Nature London* 283: 167–170, 1980.
2. BAILEY, I. A., S. R. WILLIAMS, G. K. RADDA, AND D. G. GADIAN. Activity of phosphorylase in total global ischemia in the rat heart: a ^{31}P-NMR study. *Biochem. J.* 196: 171–178, 1981.
3. BARANY, M., K. BARANY, C. T. BURT, T. GLONEK, AND T. C. MYERS. Structural changes in myosin during contraction and the state of ATP in intact frog muscle. *J. Supramol. Struct.* 3: 125–140, 1975.
4. BARANY, M., C. T. BURT, R. J. LABOTKA, M. J. DANON, T. GLONEK, AND B. H. HUNCKE. In: *Pathogenesis of Human Muscular Dystrophies*, edited by L.P. Rowland. Amsterdam: Excerpta Medica Foundation, 1977, p. 337–340.
5. BARANY, M., AND T. GLONEK. Phosphorus-31 nuclear magnetic resonance. *Methods Enzymol.* In press.
6. BESSMAN, S. P., AND P. J. GEIGER. Transport of energy in muscle: the phosphorylcreatine shuttle. *Science* 211: 448–452, 1981.
7. BROWN, T. R., D. G. GADIAN, P. B. GARLICK, G. K. RADDA, P. J. SEELEY, AND P. J. STYLES. Creatine kinase activities in skeletal and cardiac muscle measured by saturation transfer NMR. *Front. Biol. Energ.* 2: 1341–1349, 1978.
8. BROWN, T. R., AND S. OGAWA. ^{31}P-nuclear magnetic resonance kinetic measurements on adenylate kinase. *Proc. Natl. Acad. Sci. USA* 74: 3627–3631, 1977.
9. BURT, C. T., S. M. COHEN, AND M. BARANY. Analysis of intact tissue with ^{31}P-NMR. *Annu. Rev. Biophys. Bioeng.* 8: 1–25, 1979.
10. BURT, C. T., T. GLONEK, AND M. BARANY. Analysis of phosphate metabolites, the intracellular pH, and the state of adenosine triphosphate in intact muscle by phosphorus nuclear magnetic resonance. *J. Biol. Chem.* 251: 2584–2591, 1976.
11. BUSBY, S. J. W., D. G. GADIAN, G. K. RADDA, R. E. RICHARDS, AND P. J. SEELY. Phosphorus nuclear magnetic resonance studies of compartmentation in muscle. *Biochem. J.* 170: 103–114, 1978.
12. CANTOR, C. R., AND P. R. SCHIMMEL. *Biophysical Chemistry. Part II: Techniques for the Study of Biological Structure and Function.* San Francisco, CA: Freeman, 1980, p. 481–538.
13. CHANCE, B., S. ELEFF, AND J. S. LEIGH, JR. Non-invasive, nondestructive approaches to cell bioenergetics. *Proc. Natl. Acad. Sci. USA* 77: 7430–7434, 1980.
14. COHN, M., AND T. R. HUGHES, JR. Nuclear magnetic resonance spectra of adenosine di- and triphosphate. II. Effects of complexing with divalent metal ions. *J. Biol. Chem.* 237: 176–181, 1962.
15. DAWSON, M. J., D. G. GADIAN, AND D. R. WILKIE. Mechanical relaxation rate and metabolism studied in fatiguing muscle by phosphorus nuclear magnetic resonance. *J. Physiol. Lond* 299: 465–484, 1980.
16. ERECINSKA, M., AND D. F. WILSON. Homeostatic regulation of cellular energy metabolism. *Trend Biochem. Sci.* 3: 219–223, 1978.
17. FARRAR, T. C., AND E. D. BECKER. *Pulse and Fourier Transform NMR.* New York: Academic, 1971.
18. FORSEN, S., AND R. A. HOFFMANN. Study of moderately rapid chemical exchange reactions by means of nuclear magnetic double resonance. *J. Chem. Phys.* 39: 2892–2901, 1963.
19. FOSSEL, E. T., H. E. MORGAN, AND J. S. INGWALL. Measurement of changes in high energy phosphates in the cardiac cycle by using gated ^{31}P nuclear magnetic resonance. *Proc. Natl. Acad. Sci. USA* 77: 3654–3658, 1980.
20. GADIAN, D. G., AND G. K. RADDA. NMR studies of tissue metabolism. *Annu. Rev. Biochem.* 50: 69–83, 1981.
21. GADIAN, D. G., G. K. RADDA, T. R. BROWN, E. M. CHANCE, M. J. DAWSON, AND D. R. WILKIE. The activity of creatine kinase in frog skeletal muscle studied by saturation transfer nuclear magnetic resonance. *Biochem. J.* 194: 215–228, 1981.
22. GARLICK, P. B., G. K. RADDA, AND P. J. SEELEY. Studies of acidosis in the ischemic heart by phosphorus nuclear magnetic resonance. *Biochem. J.* 184: 547–554, 1979.
23. GARLICK, P. B., P. J. SEELEY, M. K. BATTERSBY, AND G. K. RADDA. Phosphorus nuclear magnetic resonance studies on perfused heart. *Regul. Mech. Carbohydr. Metab.* 42: 297–302, 1978.
24. GROVE, T. H., J. J. H. ACKERMAN, G. K. RADDA, AND P. J. BORE. Analysis of rat heart *in vivo* by phosphorus nuclear magnetic resonance. *Proc. Natl. Acad. Sci. USA* 77: 299–302, 1980.
25. GUNTHER, H. *NMR Spectroscopy: An Introduction.* New York: Wiley, 1980.
26. GUPTA, R. K., AND R. D. MOORE. ^{31}P NMR studies of intracellular free Mg^{++} in intact frog skeletal muscle. *J. Biol. Chem.* 255: 3987–3993, 1980.
27. HINSHAW, W. S., P. A. BOTTOMLEY, AND G. N. HOLLAND. Radiographic thin-section image of the human wrist by nuclear magnetic resonance. *Nature London* 270: 722–723, 1977.
28. HOLLIS, D. P. Phosphorus NMR of cells, tissues and organelles. *Biol. Magn. Reson.* 2: 1–44, 1980.
29. HOULT, D. I., S. J. W. BUSBY, D. G. GADIAN, G. K. RADDA, R. E. RICHARDS, AND P. J. SEELEY. Observation of tissue metabolites using ^{31}P nuclear magnetic resonance. *Nature London* 252: 285–287, 1974.
30. KUSHMERICK, M. J., R. A. MEYER, AND T. R. BROWN. Phosphorus NMR of cat biceps and soleus muscles. In: *Proceedings of Fifth International Symposium of International Society for Oxygen Transport to Tissues*, edited by H.I. Bicher. In press.
31. LAWSON, J. W. R., AND R. L. VEECH. Effects of pH and free Mg^{++} on the K_{eq} of the creatine kinase reaction and other phosphate hydrolyses and phosphate transfer reactions. *J. Biol. Chem.* 254: 6528–6537, 1979.
32. MCGILVERY, R. W., AND T. W. MURRAY. Calculated equilibria of phosphocreatine and adenosine phosphates during utilization of high energy phosphate by muscle. *J. Biol. Chem.* 249: 5845–5850, 1974.
33. MCLAUGHLIN, A. C., H. TAKEDA, AND B. CHANCE. Rapid ATP assays in perfused mouse liver by NMR. *Proc. Natl. Acad. Sci. USA* 76: 5445–5449, 1979.
34. MEYER, R. A., AND M. J. KUSHMERICK. Fast-twitch and slow-twitch mammalian muscles perfused *in vitro* (Abstract). *Federation Proc.* 40: 615, 1981.
35. MOON, R. B., AND J. H. RICHARDS. Determination of intracellular pH by ^{31}P nuclear magnetic resonance. *J. Biol. Chem.* 248: 7276–7278, 1973.
36. NUNNALLY, R. L., AND D. P. HOLLIS. Adenosine triphosphate compartmentation in living hearts: a phosphorus nuclear magnetic

resonance saturation transfer study. *Biochemistry* 18: 3642–3646, 1979.

37. OGAWA, S., H. ROTTENBERG, T. R. BROWN, R. G. SHULMAN, C. L. CASTILLO, AND P. GLYNN. High resolution ^{31}P-nuclear magnetic resonance study of rat liver mitochondria. *Proc. Natl. Acad. Sci. USA* 75: 1796–1800, 1978.
38. PIEPER, G. M., G. L. TODD, S. T. WU, J. M. SALHANY, F. C. CLAYTON, AND R. S. ELIOT. Attenuation of myocardial acidosis by propranolol during ischemic arrest and reperfusion: evidence with ^{31}P nuclear magnetic resonance. *Cardiovasc. Res.* 14: 646–653, 1980.
39. RADDA, G. K., AND P. J. SEELEY. Recent studies on cellular metabolism by nuclear magnetic resonance. *Annu. Rev. Physiol.* 41: 749–769, 1979.
40. ROOS, A., AND W. F. BORON. Intracellular pH. *Physiol. Rev.* 61: 296–434, 1981.
41. ROSS, B. D., G. K. RADDA, D. G. GADIAN, G. ROCKER, M. ESIRI, AND J. FALCONER-SMITH. Examination of a case of suspected McArdle's syndrome by ^{31}P nuclear magnetic resonance. *N. Engl. J. Med.* 304: 1338–1343, 1981.
42. SAKS, V. A., L. V. ROSENTRAUKH, V. N. SMIRNOV, AND E. I. CHAZOV. Role of creatine phosphokinase in cellular function and metabolism. *Can. J. Physiol. Pharmacol.* 56: 691–706, 1978.
43. SALHANY, J. M., G. M. PIEPER, S. WU, A. L. TODD, F. C. CLAYTON, AND R. S. ELIOT. ^{31}P-nuclear magnetic resonance measurements of cardiac pH in perfused guinea pig hearts. *J. Mol. Cell. Cardiol.* 11: 601–610, 1979.
44. SERAYDARIAN, K., W. F. H. M. MOMMAERTS, AND A. WALLNER. The amount and compartmentation of adenosine diphosphate in muscle. *Biochim. Biophys. Acta* 65: 443–460, 1962.
45. SHULMAN, R. G., T. R. BROWN, K. UGURBIL, S. OGAWA, S. M. COHEN, AND J. A. DEN HOLLANDER. Cellular applications of ^{31}P and ^{13}C nuclear magnetic resonance. *Science* 205: 160–166, 1979.
46. SUGDEN, P. H., AND E. A. NEWSHOLME. The effects of ammonium, inorganic phosphate and potassium ions on the activity of phosphofructokinases from muscle and nervous tissues of vertebrates and invertebrates. *Biochem. J.* 150: 113–122, 1975.
47. UGURBIL, K., H. ROTTENBERG, P. GLYNN, AND R. G. SHULMAN. ^{31}P nuclear magnetic resonance studies of bioenergetics and glycolysis in anaerobic *Escherichia coli* cells. *Proc. Natl. Acad. Sci. USA* 75: 2244–2249, 1978.
48. VEECH, R. L., J. W. R. LAWSON, N. W. CORNELL, AND H. A. KREBS. Cytosolic phosphorylation potential. *J. Biol. Chem.* 254: 6538–6547, 1979.
49. WHEELER, T. J., AND J. M. LOWENSTEIN. Adenylate deaminase from rat muscle: regulation by purine nucleotides and orthophosphate in the presence of 150 mM KCl. *J. Biol. Chem.* 254: 8994–8999, 1979.
50. WU, S. T., G. M. PIEPER, J. M. SALHANY, AND R. S. ELIOT. ^{31}P-NMR and multi-equilibria analysis of intracellular free Mg^{++} in perfused and ischemic arrested guinea pig hearts (Abstract). *Biophys. J.* 33: 26a, 1981.
51. YOSHIZAKI, K., H. NISHIKAWA, S. YAMADA, T. MORIMOTO, AND H. WATARI. Intracellualr pH measurement in frog muscle by means of ^{31}P nuclear magnetic resonance. *Jpn. J. Physiol.* 29: 211–225, 1979.

Ronald A. Meyer and Martin J. Kushmerick
Department of Physiology, Harvard Medical School Boston, Massachusetts 02115

Truman R. Brown
Bell Laboratories, Murray Hill, New Jersey 07974